

*Full Length Research Paper*

# Numerical modelling of the fluid dynamics in a bubbling fluidized bed biomass gasifier

Silva J. D.

University of Pernambuco-UPE, Polytechnic School in Recife, Rua Benfica - 455, Environmental and Energetic Technology Laboratory, Madalena, Cep: 50750-470, Recife - PE, Brazil. E-mail: [jornandesdias@poli.br](mailto:jornandesdias@poli.br).  
Tel: (081) 3184-7529, (081) 8864-8392.

Accepted 23 December, 2011

The fluid dynamics presented in this paper for a fluidized bed gasifier consists of estimating the volume fraction fields of gas and solid phases, as well as the velocity fields of gas and solid phases and the pressure drop inside the fluidized bed. However, understanding of the flow characteristics has an important role in understanding of the operation of the gasifier. The analyzed system consists of the fundamental equations of mass balance for the gas and solid phases, as well as the equations of momentum balance for gas and solid phases and an equation for the pressure given by the sum of the momentum balance equations of the gas and solid phases. The sets of equations developed form a system of one-dimensional partial differential equations (PDEs). The PDEs system has been transformed in a coupled ordinary differential equation (ODEs) system. The ODEs system has been solved using an implementation of the Runge-Kutta Gill method. The objective of this work is to obtain the profiles of state variables such as volume fraction of gas ( $\epsilon_g$ ) and solid phases ( $\epsilon_s$ ), the velocity profiles of gas ( $V_g$ ) and solid phase ( $V_s$ ) and pressure field ( $\Delta p$ ).

**Key words:** Fluid dynamics, gasifier, fluidized bed, gas-solid, biomass.

## INTRODUCTION

Gasification is a conversion of any solid or liquid fuel into an energetic gas through the process of partial oxidation due to elevated temperatures. The process of gasification occurs naturally in four distinct physical-chemical phases with temperatures of different reactions, such as the drying of biomass, devolatilization or pyrolysis, reduction and burning. Each of these processes can be analyzed in different equipment, depending on the determined sequence by the characteristics of the project.

The technique of gasification is extremely versatile but there are lots of problems in transforming this theoretical potential into a commercially competitive technology, in spite of already being practical and viable. The difficulties lie not in the basic process of gasification but in the project of a device that transforms the solid fuel into a gas of quality with trusty and security adapted to the particular conditions of the fuel and of the operation (Abdullah et al., 2003; Basu, 1999). In the case of the gases produced being used for electric energy

generation, the requirements of cleanness of these gases become of extreme necessity due to the sensitiveness of the gas turbines.

The available gasifiers can be classified in three models such as counter-current flux, for-current flux and fluidized bed. The gasifier of countercurrent flux is a device in which the pyrolyzed biomass and the air enter into different directions, the gas coming out through the upper part. The tars produced during this phase are dragged by the gases that come out from the gasifier. The biomass is gasified in the reduction zone using the energy generated in the chemical reactions that occur in the burning zone (Gabra et al., 2001a, b, c).

The co-current gasifier is characterized by the presentation of the feeding of biomass and air for the burning through the upper ending and producing gases almost tar less because the products of pyrolysis are forced through a burning zone where the biomass is found incandescent thermally destroying the tars formed resulting in clean

gases (Graham and Walsh, 1996).

The fluidized gasifier is characterized by the formation of a biomass bed in suspension produced by the effect of the flux of forced air through a distributor. The fuel particles are maintained suspended into an inert particles bed (sand, ashes, alumina, etc.), fluidized by the flux of air. The biomass is fed in reduced dimensions to allow the fluidization (Heitor and Whitelaw, 1986).

A limiting factor for this kind of equipment is the level of humidity acceptable in the biomass for the process whose limit is around 30% due to the provoked instability by the water vapor in the burning zone. This way, it becomes extremely necessary an operation of pre-drying the biomass that presents humidity superior to 30%. For small plants, this pre-drying does not show major technical or economic problems. However, for the installations of big plants that demands the handling and the storage of thousands of tons monthly and this step must be considered as an integrated part of the gasification process (Kunii and Levenspiel, 1991; Levenspiel, 2002).

Two phases can be identified in the transversal section of the bed: (i) the emulsion; (ii) the bubbles. The emulsion contains the solid particles and the gas that move (process of the filtering of the gas) through them. The flux of gas in the emulsion is limited by the minimum velocity of fluidization (Larson and Williams, 1990). Any greater amount of gas passes through the bed as bubbles. The bubbles are practically free of solid particles but in its passage through the bed, some particles are dragged by them.

The objective of this paper is to obtain the profiles of the state variables such as the volumetrical fractions of the gas ( $\varepsilon_g$ ) and solid ( $\varepsilon_s$ ) phases, velocity of the gas

phase ( $V_g$ ), velocity of the solid phase ( $V_s$ ) and the field of pressure ( $\Delta p$ ) of a fluidized bed gasifier.

## DESCRIPTION OF THE MATHEMATICAL MODEL

The applicability of the moment balance equations, energy and mass focus the sizing of gasifiers. From these balance equations, it is possible to obtain parameters that serve to characterize the process that occurs in the gasifiers. The knowledge of these optimized parameters makes the project of the equipment technically viable for an industrial scale. In the development of the model, some hypothesis were considered: (i) the fluxes are one-dimensional, (ii) the fluid phase is compressible, (iii) all the particles have the same dimension; (iv) the irregular movement and the colliding of the particles are ignored; (v) the friction on the wall is ignored. Having said that, based on these hypothesis it was developed the following fluid dynamic model for the balances of mass and moment:

Mass balance for the gas phase:

$$\frac{\partial \varepsilon_g}{\partial t} + V_g \frac{\partial \varepsilon_g}{\partial z} = (1 - \varepsilon_s) \frac{g}{V_g} \quad (1)$$

Mass balance for the solid phase:

$$\frac{\partial \varepsilon_s}{\partial t} + V_s \frac{\partial \varepsilon_s}{\partial z} = (1 - \varepsilon_g) \frac{g}{V_s} \quad (2)$$

Moment balance for the gas phase:

$$\rho_g \left( \varepsilon_g \frac{\partial V_g}{\partial t} + 2 \varepsilon_g V_g \frac{\partial V_g}{\partial z} \right) = - \rho_g \left( V_g \frac{\partial \varepsilon_g}{\partial t} + V_g^2 \frac{\partial \varepsilon_g}{\partial z} \right) - (1 - \varepsilon_s) \frac{\partial P}{\partial z} - \varepsilon_g \rho_g g - F_s \quad (3)$$

Moment balance for the solid phase:

$$\rho_s \left( \varepsilon_s \frac{\partial V_s}{\partial t} + 2 \varepsilon_s V_s \frac{\partial V_s}{\partial z} \right) = - \rho_s \left( V_s \frac{\partial \varepsilon_s}{\partial t} + V_s^2 \frac{\partial \varepsilon_s}{\partial z} \right) - (1 - \varepsilon_g) \frac{\partial P}{\partial z} - \varepsilon_s \rho_s g - F_s \quad (4)$$

The addition of Equations (3) and (4) results in an only equation for the pressure drop, being expressed as:

$$-\frac{\partial P}{\partial z} = \rho_s \left[ \left( \varepsilon_s \frac{\partial V_s}{\partial t} + V_s \frac{\partial \varepsilon_s}{\partial z} \right) + \left( \frac{\partial V_s}{\partial z} 2 \varepsilon_s V_s + V_s^2 \frac{\partial \varepsilon_s}{\partial z} \right) \right] + \rho_g \left[ \left( \varepsilon_g \frac{\partial V_g}{\partial t} + V_g \frac{\partial \varepsilon_g}{\partial z} \right) + \left( \frac{\partial V_g}{\partial z} 2 \varepsilon_g V_g + V_g^2 \frac{\partial \varepsilon_g}{\partial z} \right) \right] + (\rho_g \varepsilon_g + \rho_s \varepsilon_s) g \quad (5)$$

in which:

$$F_s = \frac{(\rho_s - \rho_g) g \varepsilon_g (1 - \varepsilon_s)^{(1-n)} (v_g - v_s)}{v_t}; v_t = \left( \frac{\rho_s - \rho_g}{\rho_s} \right) g \tau \text{ and}$$

$$\tau = \frac{d_p^2 \rho_s}{k \mu_g}$$

The initial and boundary conditions of equations (1) to (5) are given in Table 1.

### SOLUTION OF THE SIMULATION MODEL

Equations of the model together with the initial and boundary conditions form a coupled partial differential equation system (PDEs), which characterizes a problem of initial values and boundary. These equations of model are very complex to be solved analytically. Having said that, it was used the methods of the lines (ML) to solve the system of PDEs. This method discretizes the partial

derivades for method such as finite differences orthogonal collocation etc, forming a system of ODEs.

The system of ODEs will be solved with the implementation of Runge-Kutta Gill's method (Rice and Duong, 1995). In this present paper, this methodology was used:

Mass balance for the gas phase, discretized:

$$\frac{d\varepsilon_g}{dt} = \left[ 1 - (\varepsilon_s)_j^{(k)} \right] \frac{g}{(V_g)_j^{(k)}} - \frac{2(V_g)_j^{(k)}}{\Delta z} \left[ \varepsilon_{g,0} - (\varepsilon_g)_j^{(k)} \right] \quad (6)$$

Mass balance for the solid phase, discretized:

$$\frac{d\varepsilon_s}{dt} = \left[ 1 - (\varepsilon_g)_j^{(k)} \right] \frac{g}{(V_s)_j^{(k)}} - \frac{2(V_s)_j^{(k)}}{\Delta z} \left[ \varepsilon_{s,0} - (\varepsilon_s)_j^{(k)} \right] \quad (7)$$

Moment balance for the gas phase, discretized:

$$-\frac{dV_g}{dt} = \frac{\left[ 1 - (\varepsilon_s)_j^{(k)} \right]}{(\varepsilon_g)_j^{(k)}} \left\{ g + \frac{2}{\rho_g \Delta z} \left[ P_0 - (P)_j^{(k)} \right] \right\} \frac{4(V_g)_j^{(k)}}{\Delta z} \left[ V_{g,0} - (V_g)_j^{(k)} \right] + \frac{(F_s)_j^{(k)}}{\rho_g (\xi_g)_j^{(k)}} \quad (8)$$

Moment balance for the solid phase, discretized:

$$-\frac{dV_s}{dt} = \frac{\left[ 1 - (\varepsilon_g)_j^{(k)} \right]}{(\varepsilon_s)_j^{(k)}} \left[ g + \frac{2}{\rho_s \Delta z} \left[ P_0 - (P)_j^{(k)} \right] \right] + \frac{4(V_s)_j^{(k)}}{\Delta z} \left[ V_{s,0} - (V_s)_j^{(k)} \right] + \frac{(F_s)_j^{(k)}}{\rho_s (\xi_s)_j^{(k)}} + g \quad (9)$$

Pressure drop, discretized

$$-\frac{dP}{dz} = \rho_s \left\{ \begin{array}{l} -g \left[ 1 - (\varepsilon_g)_j^{(k)} \right] - \frac{2 \left[ 1 - (\varepsilon_g)_j^{(k)} \right]}{\rho_s \Delta z} \left[ P_0 - (P)_j^{(k)} \right] \\ \frac{(F_s)_j^{(k)}}{\rho_s} + \frac{2(V_s)_j^{(k)}}{\Delta z} \left[ \xi_{s,0} - (\varepsilon_s)_j^{(k)} \right] \left[ 1 + (V_s)_j^{(k)} \right] \end{array} \right\} + \rho_g \left\{ \begin{array}{l} -g \left[ 1 - (\varepsilon_s)_j^{(k)} \right] - \frac{2 \left[ 1 - (\varepsilon_s)_j^{(k)} \right]}{\rho_g \Delta z} \left[ P_0 - (P)_j^{(k)} \right] \\ \frac{(F_s)_j^{(k)}}{\rho_g} + \frac{2(V_g)_j^{(k)}}{\Delta z} \left[ \varepsilon_{g,0} - (\varepsilon_g)_j^{(k)} \right] \left[ 1 + (V_g)_j^{(k)} \right] \end{array} \right\} \quad (10)$$

Where: 
$$F_s = \frac{(\rho_s - \rho_g) g (\varepsilon_g)_j^k \left[ 1 - (\varepsilon_s)_j^k \right]^{(1-n)} \left[ (v_g)_j^k - (v_s)_j^k \right]}{v_t}$$

**Table 1.** Initial and boundary conditions.

Initial conditions	Boundary conditions
$\varepsilon_g _{t=0} = 0$	$\varepsilon_g _{z=0^+} = \varepsilon_{g,0}$
$\varepsilon_s _{t=0} = 0$	$\varepsilon_s _{z=0^+} = \varepsilon_{s,0}$
$V_g _{t=0} = 0$	$V_g _{z=0^+} = V_{g,0}$
$V_s _{t=0} = 0$	$V_s _{z=0^+} = V_{s,0}$
—	$P _{z=0^+} = P_0$

**Table 2.** Parameters used in the simulation.

Parameter	Unit
$\rho_s = 1,21$	$kg.m^{-3}$
$\rho_g = 1150$	$kg.m^{-3}$
$\mu_g = 1,8 \times 10^{-5}$	$Pa.s$
$g = 9,8$	$m.s^{-2}$
$d_g = 500$	$\mu m$
$n = 1,37$	-
$k = 0,8$	-
$\Delta t = 10^{-2}$	$s$

**RESULTS AND DISCUSSIONS**

The solution of the developed model provided the behavior of the volumetric fraction of the gas phase ( $\varepsilon_g$ ), volumetric fraction of the solid phase ( $\varepsilon_s$ ), velocity of the gas phase ( $V_g$ ), velocity of the gas phase ( $V_s$ ) and pressure drop ( $\Delta P$ ) versus the time in the exit of the burning zone of the fluidized bed gasifier. The data used for the feeding of the computer code developed are presented in Table 2.

A model validation procedure was established by comparing between the model for the superficial velocity of the gas phase and Sirinivasan and Angirasa (1988) according to Figure 1. Figures 2 and 3 show a dynamic evolution of the volumetric fractions (eg and es) at  $z = H$ . It is observed that there was an increase of these fractions with the increase of the parameter  $\varepsilon_{g,0}$  at the inlet of the system. The volumetric fractions will encounter an invariable state around  $t = 100$ . The two fractions presented the very similar results. Figures 4 and 5 show the dynamic evolution of the velocities in the gas and

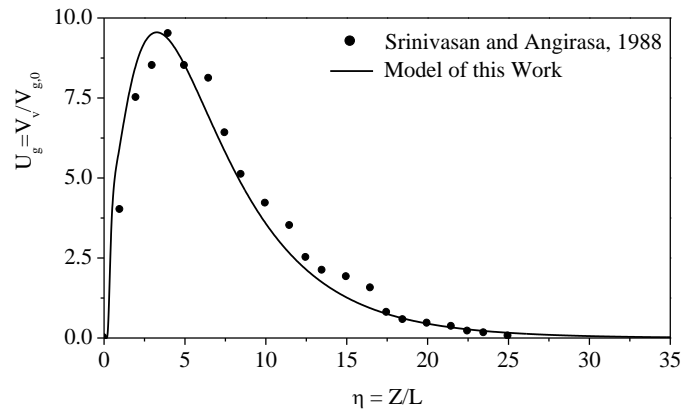


**Figure 1.** Comparisons of dimensionless curves for the solution of the model for the superficial velocity of the gas phase and Sirinivasan and Angirasa (1988).

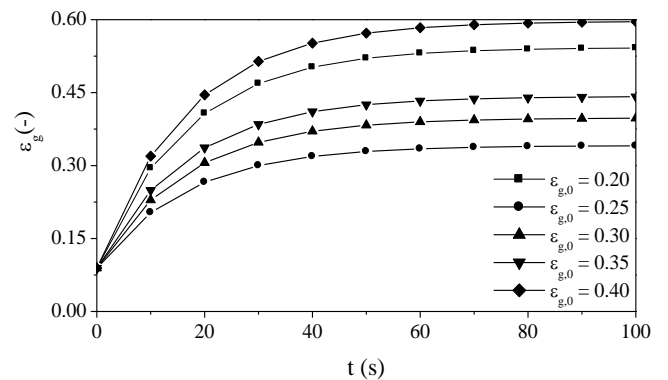


**Figure 2.** Profiles of the volumetric fraction of the gas phase in the exit of the fluidized bed gasifier countercurrent with the length at 1 m.

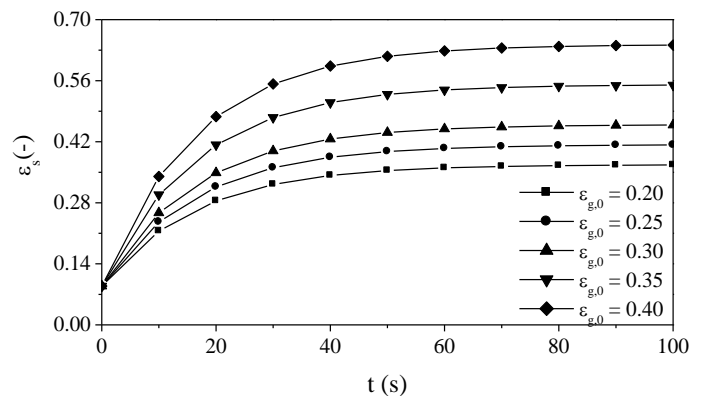


**Figure 3.** Profiles of volumetric fraction in the solid phase in the exit of the fluidized bed gasifier countercurrent with the length at 1 m.

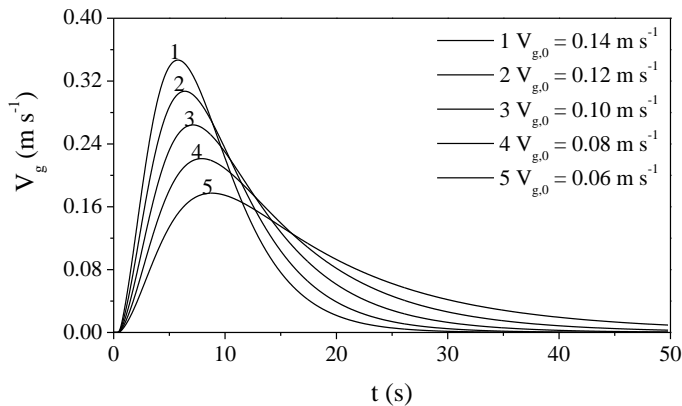


**Figure 4.** Profiles of the superficial velocity of the gas phase in the exit of the bubbling fluidized bed gasifier countercurrent with the length at 1 m.

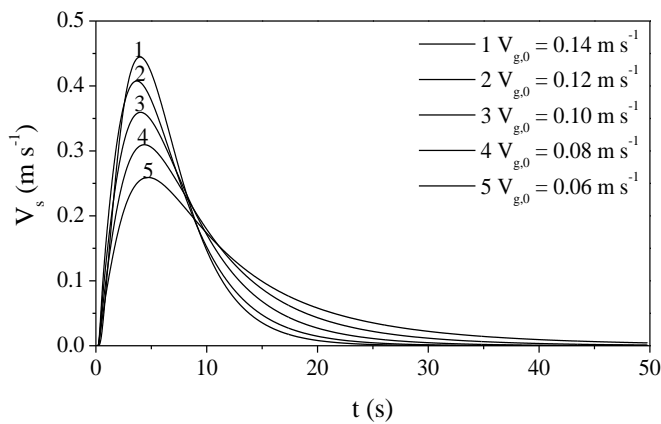


**Figure 5.** Profiles of the superficial velocity of the solid phase in the exit of the bubbling fluidized bed gasifier countercurrent with the length at 1 m.

solid phases ( $V_g$  and  $V_s$ ) at  $z = H$ . The graphs show that such velocities also suffered substantial increase with the rising of variable  $V_{g,0}$  at the inlet but from 30 to 50 s in the velocity  $V_g$  and from 25 to 50 s in the velocity  $V_s$  there was a fall until zero. It could also be observed that with the rising at the inlet variable  $V_{g,0}$  the fall of the velocities ( $V_g$  and  $V_s$ ) were quicker.

Figure 6 shows a pressure field along the region of fluidization. It is observed the effect of velocity  $V_{g,0}$  at the inlet under the pressure inside the fluidized bed showing in the graph that the velocity was proportional to the rising of the pressure until zero.

## Conclusion

The modelling of the gas-solid process of the fluidized

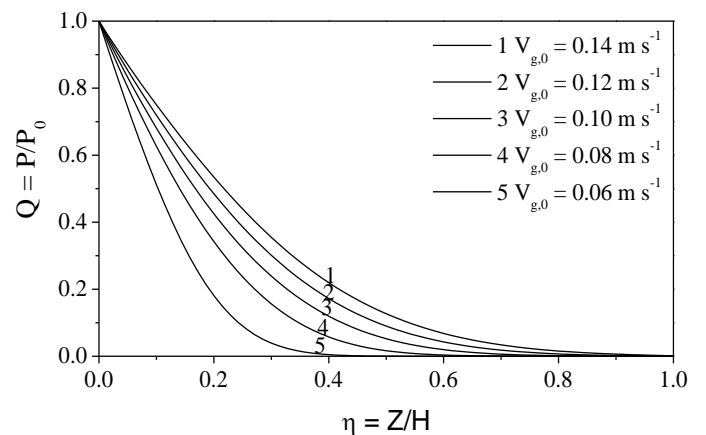


**Figure 6.** Profiles of the pressure drop in the bubbling fluidized bed gasifier countercurrent with the length at 1 m.

bed was developed in relation to the volumetric fractions ( $\epsilon_g$  and  $\epsilon_s$ ) and the velocities ( $V_g$  and  $V_s$ ) as well as an equation for the pressure drop resulting from the adding of equations  $V_g$  and  $V_s$ . The simulations of this model led us to the following conclusions:

- i. The validation portrayed a satisfactory prognostication for the numerical experiment conducted for the variable  $V_{g,0}$ ;
- ii. It was allowed by the developed model to analyze the sensitivity of the variables  $\epsilon_g$  and  $\epsilon_s$  with the variable  $\epsilon_{g,0}$ , at the inlet, as well as the variables  $V_g$ ,  $V_s$  and  $p$  by using the variable at the inlet  $V_{g,0}$ ;
- iii. It was shown by the variables  $\epsilon_{g,0}$  and  $V_{g,0}$  at the inlet, great influence on the behavior of the fluidynamic variables of the gas-solid process concerning the control of the process in this equipment;
- iv. In this paper, it was performed using simulations only with  $\epsilon_{g,0}$  and  $V_{g,0}$  of feeding. However, other variables at the inlet can be tested.

## ACKNOWLEDGEMENT

The author would like to thank CNPQ (National Council of Scientific and Technological Development) for the financial support given (Process 48354 / 2007 / Project / Title: Computer Modeling and Simulation for the Development of the technology of a Gasification Plant in Combined Cycle for the Generation of Electric Energy./Edict CNPq 15/2007 – Universal).

## Nomenclature

$D_p$ : Diameter of the particles, m

$F_s$ : Force of interaction between the gas and solid phases per volume unit,  $\text{kg s}^{-2} \text{m}^{-2}$

G: Gravity acceleration,  $\text{m s}^{-2}$   
 H: Length of the fluidization zone, m  
 K: Constant of equation (9)  
 N: Constant of equation (10)  
 P: Pressure, Pa  
 $P_0$ : Initial pressure, Pa  
 Q: Dimensionless pressure  
 T: Temporal coordinate, s  
 $V_g$ : Velocity of the gas phase,  $\text{m s}^{-1}$   
 $V_{g,0}$ : Velocity of the initial gas phase,  $\text{m s}^{-1}$   
 $V_s$ : Velocity of the solid phase,  $\text{m s}^{-1}$   
 $V_t$ : Ending velocity of the liquid particle,  $\text{m s}^{-1}$   
 U: Dimensionless Velocity  
 Z: Special coordinate, m

### Greek letters

$\epsilon_g$ : Volumetric fraction of the gas phase  
 $\epsilon_{g,0}$ : Volumetric fraction of the initial gas phase  
 $\epsilon_s$ : Volumetric fraction of the solid phase  
 $\mu_g$ : Coefficient of viscosity of the gas phase, Pa s  
 $\rho_g$ : Density in the gas phase,  $\text{kg m}^{-3}$   
 $\rho_s$ : Density in the solid phase,  $\text{kg m}^{-3}$   
 $\tau$ : Factor of relaxation ( $0 \leq \tau \leq 1$ ) for the gas phase, s  
 $\Delta t$ : Time pace, s

### REFERENCES

- Abdullah MZ, Husam Z, Yin PSL (2003). "Analysis of coal flow fluidization test results for various biomass fuels, *Biomass Bioenergy*, 24: 487-494.
- Basu P (1999). "Combustion of coal circulating fluidized-bed boilers: a review." *Chem. Eng. Sci*, 54: 5545-555.
- Gabra M, Nordin A, Ohman M, Kjellstrom B (2001c) "Alkali retention/separation during bagasse gasification: a comparison between a fluidized bed and a cyclone gasifier". *Biomass Bioenergy*, 21: 461-476.
- Gabra M, Pettersson E, Backman R, Kjellstrom B (2001a) "Evaluation of cyclone gasifier performance for gasification of sugar cane residue-Part I: gasification of bagasse". *Biomass Bioenergy*, 21: 351-369.
- Gabra M, Pettersson E, Backman R, Kjellstrom B (2001b). "Evaluation of cyclone gasifier performance for gasification of sugar cane residue-Part I: gasification of cane trash". *Biomass Bioenergy*, 21: 371-380.
- Graham RL, Walsh ME (1996). "Evaluating the economic costs, benefits and tradeoffs of dedicated biomass energy systems: the importance of scale", In: *Second Biomass Conference of the Americas: Energy, Environment, Agriculture, and Industry*, Portland, Oregon, pp. 207-215.
- Heitor MV, Whitelaw JH (1986). "Velocity temperature and species characteristics of the on in a gas turbine combustor", *Combust. Flame*, 1: 64-76.
- Kunii D, Levenspiel O (1991). "Fluidization Engineering", second ed., Butterworth-Heinemann, Boston, pp. 137-164.
- Larson ED, Williams RH (1990). "Biomass-Gasifier Steam-Injected Gas Turbine Cogeneration". *J. Engine. Gas Turbines Power*, 112: 157-163.
- Levenspiel O (2002). "Modeling in chemical engineering". *Chem. Eng. Sci.*, 57: 4691-4696.
- Rice RG, Duong DD (1995). "Applied mathematics and modeling for chemical engineers, John Wiley & Sons, Inc, United States, pp. 706.
- Srinivasan J, Angirasa D (1988). "Numerical study of double-diffusive free convection from a vertical surface". *Int. J. Heat, Mass Transfer*, 31: 2033-2038.